Absorption of higher-order modes in millimeter-wave waveguides using graphene sheets

S. A. Amanatiadis, G. D. Bouzianas, N. V. Kantartzis, and T. D. Tsiboukis

Department of Electrical and Computer Engineering
Aristotle University of Thessaloniki
GR-54124 Thessaloniki, Greece
Fax: + 30-2310-996312; email: tsibukis@auth.gr

Abstract

An efficient technique for the design of millimeter-wave, graphene-loaded waveguides that prevent the propagation of selected higher-order modes and do not allow a significant energy portion to be reflected back to the source plane, is developed in this paper. The optimal location of graphene films is obtained via the theoretical calculation of the electromagnetic field pattern inside the waveguide.

1. Introduction

Rectangular waveguides are commonly used for the propagation of electromagnetic energy at microwave and millimeter-wave frequencies. The upper limit of the waveguide's operation bandwidth is determined by the cut-off frequency of its higher-order modes. To this aim, a variety of means for the absorption of these modes has been proposed over the recent years [1].

In this paper, a new non-destructive method which incorporates thin graphene layers is presented for the suppression of higher-order modes and the concurrent reduction of the reflection coefficient, as well. The key asset of our concept stems from the unique properties of graphene, which is an one-atom thick planar material comprising carbon atoms bonded in a hexagonal structure [2]. Although its overall contribution so far focuses mainly at optical frequencies [3], its electromagnetic behavior at the millimeter-wave region should be seriously taken into account, since it can offer various beneficial design perspectives.

2. Theoretical aspects of graphene and waveguide structures

For our analysis, graphene sheets are modeled as infinitesimally thin, local two-sided layers characterized by a surface conductivity $\sigma(\omega, \mu_c, \Gamma, T)$, where ω is the radian frequency, μ_c the chemical potential controlled by a gate voltage or chemical doping, Γ a phenomenological scattering rate assumed to be independent of energy, and T the temperature. In this context, graphene's conductivity is evaluated by the subsequent expression, resulting from the Kubo formula [4],

$$\sigma(\omega, \mu_c, \Gamma, T) = \frac{\jmath e^2(\omega - \jmath 2\Gamma)}{\pi \hbar^2} \left[\frac{1}{(\omega - \jmath 2\Gamma)^2} \int_0^\infty \varepsilon \left(\frac{\partial f_d(\varepsilon)}{\partial \varepsilon} - \frac{\partial f_d(-\varepsilon)}{\partial \varepsilon} \right) \mathrm{d}\varepsilon \right.$$
$$\left. - \int_0^\infty \frac{f_d(-\varepsilon) - f_d(\varepsilon)}{(\omega - \jmath 2\Gamma)^2 - 4(\varepsilon/\hbar)^2} \mathrm{d}\varepsilon \right], \qquad (1)$$

with $-e$ the electron's charge, $\hbar$ the reduced Planck's constant, $f_d = [e^{(\varepsilon-\mu_c)/k_B T} + 1]^{-1}$ the Fermi-Dirac distribution, and k_B the Boltzmann's constant. At the frequencies of our interest, the first term in (1) is the dominant one, essentially due to the intraband contributions, and can be computed via

$$\sigma_{intra}(\omega, \mu_c, \Gamma, T) = -\jmath \frac{e^2 k_B T}{\pi \hbar^2 (\omega - \jmath 2\Gamma)} \left[\frac{\mu_c}{k_B T} + 2 \ln \left(e^{-\mu_c/k_B T} + 1 \right) \right]. \qquad (2)$$

ISBN 978-952-67611-2-1 © 2012 Metamorphose VI

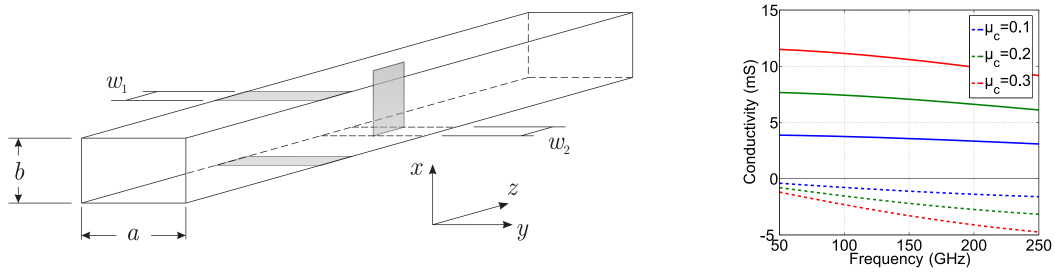

(a) (b)

Fig. 1: (a) Setup of the waveguide system and (b) real (solid lines) and imaginary (dashed lines) part of graphene's conductivity for three different chemical potentials μ_c versus frequency.

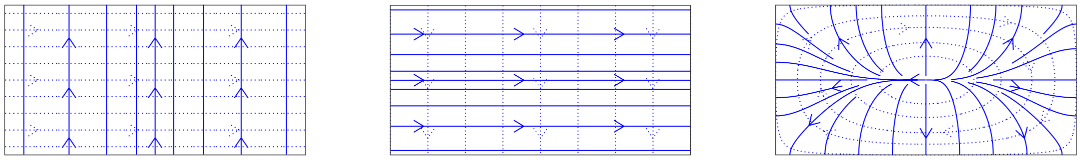

(a) (b) (c)

Fig. 2: Electric (solid lines) and magnetic (dashed lines) field inside a rectangular waveguide for the (a) TE_{10} (b) TE_{01}, and (c) TM_{11} mode.

Assuming a uniform waveguide of rectangular cross-section with a propagation direction along the positive z-axis, as depicted in Fig. 1(a), electric and magnetic field vectors can be calculated by the Helmholtz equation by means of the appropriate boundary conditions. In this manner, field amplitudes inside the waveguide for the transverse electric modes (TE_{mn}) are given by

$$\dot{\boldsymbol{E}}_{mn} = \left(\frac{\jmath q \mu \omega}{p^2+q^2} \; \cos px \;\, \sin qy \; \hat{\mathbf{x}} - \frac{\jmath p \mu \omega}{p^2+q^2} \; \sin px \;\, \cos qy \; \hat{\mathbf{y}} \right) H_o \; e^{-\jmath\beta z}, \tag{3}$$

$$\dot{\boldsymbol{H}}_{mn} = \left(\frac{\jmath \beta p}{p^2+q^2} \; \sin px \;\, \cos qy \; \hat{\mathbf{x}} + \frac{\jmath \beta q}{p^2+q^2} \; \cos px \;\, \sin qy \; \hat{\mathbf{y}} + \cos px \;\, \cos qy \; \hat{\mathbf{z}} \right) H_o \; e^{-\jmath\beta z}, \tag{4}$$

where $\beta = \sqrt{\omega^2 \mu \varepsilon - p^2 - q^2}$ is the propagation constant with $p = \frac{m\pi}{a}$ and $q = \frac{n\pi}{b}$, ε is the permittivity, and μ the permeability of the medium. Likewise, the amplitude of electric and magnetic fields for the transverse magnetic modes (TM_{mn}) can be expressed as

$$\dot{\boldsymbol{E}}_{mn} = \left(-\frac{\jmath \beta p}{p^2+q^2} \; \cos px \;\, \sin qy \; \hat{\mathbf{x}} - \frac{\jmath \beta q}{p^2+q^2} \; \sin px \;\, \cos qy \; \hat{\mathbf{y}} + \sin px \;\, \sin qy \; \hat{\mathbf{z}} \right) E_o \; e^{-\jmath\beta z}, \tag{5}$$

$$\dot{\boldsymbol{H}}_{mn} = \left(\frac{\jmath q \varepsilon \omega}{p^2+q^2} \; \sin px \;\, \cos qy \; \hat{\mathbf{x}} - \frac{\jmath p \epsilon \omega}{p^2+q^2} \; \cos px \;\, \sin qy \; \hat{\mathbf{y}} \right) E_o \; e^{-\jmath\beta z}. \tag{6}$$

The necessary adjustment of the aforementioned graphene sheets inside the waveguide depends on the pattern of the electromagnetic field at a plane perpendicular to the propagation axis. For illustration, the field patterns of three different modes at such a plane are shown in Fig. 2, where the electric field is plotted with solid lines and the magnetic field with dashed lines.

3. Developement of the design method and numerical results

In order to initiate our design, three graphene sheets are placed inside the waveguide, as described in Fig. 1(a). The first two are set at the waveguide boundaries and are intended to attenuate the selected modes. Actually, this attenuation occurs due to the excitation of surface currents on the layers of graphene, generated by magnetic field tangential components. The third sheet operates as a reflector and is parallel to the electric field lines of the mode that is to be suppressed, i.e. TE_{01} in this paper. It is

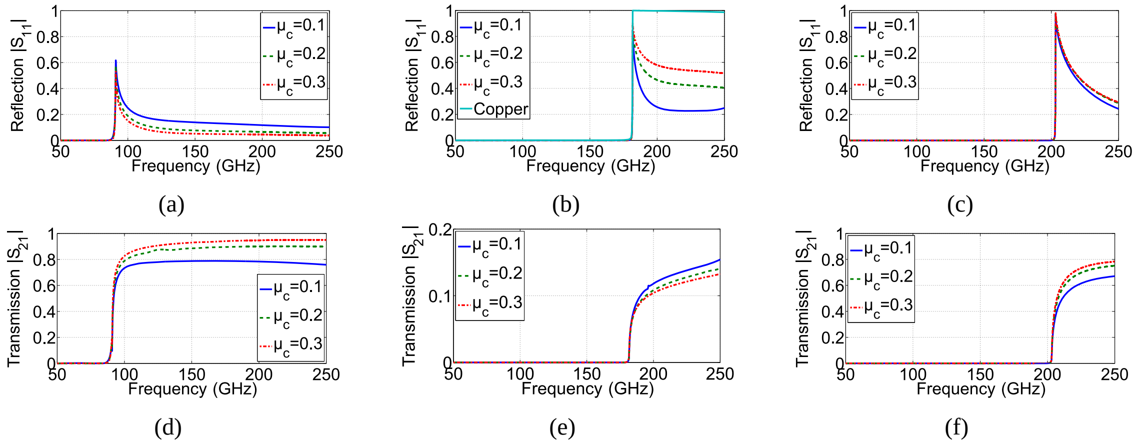

Fig. 3: Reflection $|S_{11}|$ and transmission $|S_{21}|$ of (a), (d) TE_{10} (b), (e) TE_{01}, and (c), (f) TM_{11} modes.

interesting to mention that reflected waves are additionally faded, because of the first two graphene films locates at the waveguide edges. Evidently, all TE modes, including the dominant one, are influenced by the proposed graphene configuration, a fact which is mainly attributed to the magnetic field component parallel to the propagation direction. Hence, dimensions w_1 and w_2 in Fig. 1(a) have to be carefully chosen, while TM modes may be protected through the optimal position of graphene layers.

Let us consider an empty WR-6 millimeter-wave waveguide with cross-section dimensions of $a = 1.651\,\text{mm}$ and $b = 0.8255\,\text{mm}$. The conductivity of graphene versus the desired frequency range is displayed in Fig. 1(b) with $\Gamma = 1\,\text{meV}$, room's temperature $T = 300\,\text{K}$, and three different chemical potentials μ_c, while $w_1 = 0.3\,\text{mm}$ and $w_2 = 0.5\,\text{mm}$. The transmission and reflection coefficients of the waveguide modes, so attained, are extracted via a typical finite-element approach. Moreover, Fig. 3 shows the simulation results which clearly certify that the dominant TE_{10} mode is only slightly affected, especially near the cut-off frequency, due to the aforesaid surface current on the graphene sheets. In contrast, the transmission of the TE_{01} mode is sufficiently suppressed, whereas the overall reflection is also adequately decreased, as compared to the case where a copper film is utilized (cyan line in Fig. 3(b)). In this manner, the source plane of the structure is properly protected. Finally, it can be observed from Fig. 3 that the TM_{11} mode is somewhat degraded because of the non-optimized graphene location.

4. Conclusion

A rectangular waveguide structure at millimeter-wave frequencies combined with graphene layers for the annihilation of specific higher-order modes, is designed in this paper via a novel non-destructive technique. The correct position of the graphene sheets is achieved according to their conductivity profile and the field pattern of the respective modes. Numerical results, extracted through a finite-element algorithm substantiate that the transmission of the selected mode is interrupted with a satisfactory reduction of the reflected wave power, while the propagation of the dominant TE_{10} mode, is trivially affected.

Acknowledgment

This research has been co-financed by the EU (European Social Fund – ESF) and Greek national funds through the Operational Program "Education and Lifelong Learning" of the National Strategic Reference Framework (NSRF) – Research Funding Program: ARISTEIA I. Investing in knowledge society through the European Social Fund.

References

[1] D. Lioubtchenko, S. Tretyakov, and S. Dudorov, *Millimeter-Wave Waveguides*, Heidelberg, Germany: Springer, 2003.
[2] A. Geim and K. Novoselov, The rise of graphene, *Nature Materials*, vol. 6, no. 3, pp. 183–191, 2007.
[3] A. Vakil and N. Engheta, Transformation optics using graphene, *Science*, vol. 332, no. 6035, p. 1291, 2011.
[4] V. Gusynin, S. Sharapov, and J. Carbotte, Magneto-optical conductivity in graphene, *Journal of Physics: Condensed Matter*, vol. 19, pp. 026222(1–25), 2007.